0013-7227/03/$15.00/0
Printed in U.S.A.

Endocrinology 144(3):1045–1052

doi: 10.1210/en.2002-220823

Divergent Expression of Type 2 Deiodinase and the Putative Thyroxine-Binding Protein p29, in Rat Brain, Suggests that They Are Functionally Unrelated Proteins

ANA MONTERO-PEDRAZUELA, JUAN BERNAL, AND ANA GUADAÑO-FERRAZ

Instituto de Investigaciones Biomédicas "Alberto Sols," Consejo Superior de Investigaciones Científicas-Universidad Autónoma de Madrid, 28029 Madrid, Spain

Deiodinases (D1, D2, and D3) are selenoproteins involved in thyroid hormone metabolism. Generation of the active hormone T_3, from T_4, is carried out by D1 and D2, whereas D3 degrades both hormones. The identity of the cloned D2 as a selenoprotein is well supported by biochemical and physiological data. However, an alternative view has proposed that type 2 deiodinase is a nonselenoprotein complex containing a putative T_4 binding subunit called p29, with an almost identity in sequence with the Dickkopf protein Dkk3.

To explore a possible functional relationship between p29 and D2, we have compared their mRNA expression patterns in the rat brain. In brain, parenchyma p29 was expressed in neurons. High expression levels were found in all the regions of the blood-cerebrospinal fluid (CSF) barrier. p29 was present in different types of cells than D2, with the exception of the tanycytes. Our data do not support that p29 has a functional relationship with D2. On the other hand, expression of p29 in the blood-CSF barrier suggests that it might be involved in T_4 transport to and from the CSF, but further studies are needed to substantiate this hypothesis. (*Endocrinology* 144: 1045–1052, 2003)

DEIODINASES ARE A FAMILY of selenoproteins involved in thyroid hormone (TH) metabolism and, specifically, in generation of T_3 from T_4 and degradation of iodothyronines [reviewed by Bianco *et al.*, 2002 (1); Leonard and Köhrle, 2000 (2); Köhrle, 1999 (3); and Leonard and Visser, 1986 (4)]. Three deiodinases have been identified and cloned (5–7) and are known as type 1 (D1), type 2 (D2), and type 3 (D3) deiodinases. Generation of the active hormone T_3 from T_4 in target tissues is performed by D1 and D2. In rodents, D1 and D2 have similar contributions to circulating T_3. D2 is additionally involved in the intracellular generation of T_3 in target tissues such as brain, pituitary and brown adipose tissue. In humans, D2 is also expressed in skeletal muscle and may also contribute to circulating T_3 (8). Degradation of T_4 and T_3 to reverse T_3 and 3,3′diiodothyronine, respectively, is carried out by D1 and D3 (9).

Deiodinases are selenoproteins, which contain the rare amino acid selenocysteine. The selenoprotein mRNAs contain a bifunctional UGA codon that signals either the usual stop codon, or the amino acid selenocysteine. For the latter function, it needs Se and a special sequence in the 3′-untranslated region called the selenocysteine insertion sequence element. The selenoprotein nature of D1 and D3 has not been a matter of discussion (7, 10, 11). Concerning D2, the identification of a selenocysteine insertion sequence element in the human D2 (12), robust biochemical data (13), and results from knockout animals (14) solidly support the identity of the cloned D2 as a physiological selenoprotein with D2 activity. Despite this, an alternative view has proposed that D2 is a nonselenoprotein, multiprotein complex of about 200 kDa consisting of catalytic and T_4-binding subunits (15, 16). Furthermore, the cloned D2 mRNA would not encode the physiological enzyme. Reasons to support these views include a lack of effect of Se deficiency on D2 activity (17–19), the low inhibition of type 2 deiodinase activity by gold in contrast with other selenoproteins (20), and the failure to detect any protein with antibodies generated from the conceptual translation of the cloned D2 cDNA (21). Along this reasoning, a putative T_4-binding subunit identified by affinity labeling as a 29-kDa protein (p29) was recently cloned from rat (22). The cDNA encoding p29 has a high degree of similarity to members of the Dickkopf (Dkk-1–4) family of secreted glycoproteins involved in regulation of dorsoventral patterning during embryonic development (23, 24). In particular, rat p29 has 87% similarity at the nucleotide level with mouse Dkk-3, a protein with tumor suppressor activity (25) expressed at higher levels in heart, brain and spinal cord (23). Data supporting a role for p29 in TH metabolism include the enhancement of D2 activity when transfected to cultured astrocytes (22).

Expression of D2 is particularly important in the brain given the developmental effects of TH and the fact that most T_3 present in brain is formed locally from T_4 because of D2 activity (26). Expression and activity of D2 in brain are regulated by TH concentrations such that they increase in hypothyroidism and decrease in hyperthyroidism as a compensatory mechanism to maintain normal T_3 concentrations (27–31). D2 is expressed predominantly in astrocytes and, in much higher amounts, in the tanycytes lining the walls of the third ventricle (32, 33). Expression of D2 mRNA correlates with deiodinase activity measured in punches from different brain regions (34). We reasoned that, if there is any functional relationship between p29 as a putative T_4-binding subunit of

Abbreviations: CSF, Cerebrospinal fluid; D1–D3, deiodinases types 1–3; Dkk, Dickkopf; p29, 29-kDa protein; TH, thyroid hormone; UTP, uridine triphosphate.

a deiodinase multiprotein complex and D2, the expression of both molecular species would show a large degree of overlap among regions and cell types of brain tissue. To this end, we have simultaneously analyzed the distribution of p29 and D2 mRNAs by *in situ* hybridization. Our results indicate that p29 is expressed in different types of cells than D2, with the notable exception of the tanycytes. p29 is expressed with a neuronal-like distribution and is also found in cells of the blood-CSF barrier. Our data do not support that p29 has a functional relationship with D2, but open the possibility that it may be involved in T_4 transport to and from the CSF contributing to T_4 availability within the brain.

Materials and Methods

Animals and treatments

Male Wistar rats 16 and 60 d old (P16 and P60) were used in these studies. In addition, hypothyroid male Wistar P16 rats were used. To induce hypothyroidism, pregnant dams were given 0.02% 2-mercapto-1-methylimidazole (Sigma, St. Louis, MO) and 1% sodium perchlorate in the drinking water *ad libitum* from gestational d 10 and throughout lactation until the neonates were killed at P16. This protocol causes severe hypothyroidism as shown by reduced growth rate and large decreases of T_4 and T_3 concentrations in serum and cerebral cortex (35). Animals were under temperature (22 ± 2 C) and light (12-h light, 12-h dark cycle; lights on at 0700 h) controlled conditions and had free access to food and water. Animal care procedures were conducted in accordance with the guidelines set by the European Community Council Directives (86/609/EEC).

Tissue processing

Rats were anesthetized by ip injection of a mixture of Ketamine (4 mg/100 g body weight) and Metedomidine (15 mg/100 g body weight), and the animals were perfused transcardially with fixative [4% paraformaldehyde in 0.1 M phosphate buffer, pH 7.4]. Brains were removed, post fixed in the same solution overnight, and cryoprotected at 4 C for 2–3 d in the paraformaldehyde solution containing 30% sucrose. They were then frozen in dry ice and coronal sections 25 μm thick were obtained in a cryostat. The sections were stored at −70 C in a cryoprotective solution containing 30% ethylenglycol, 30% glycerol, and 40% 0.1 M phosphate buffer.

RNA probes

A specific p29 probe (nucleotides 1172–1499, 327 bp) was designed based on the published rat cDNA sequence (accession no. AF245040) (22), and the DNA template isolated by RT-PCR. Total cerebral cortex RNA was isolated from P16 rats using TRIzol reagent (Life Technologies, Inc.) according to the manufacturer's instructions. The cDNA was obtained with the cDNA synthesis kit (Amersham Pharmacia Biotech, Buckinghamshire, UK). The following primers were used to amplify the p29 specific sequences: forward (1172–1191), 5′-CTTGA CAAGG TACAG TGCAG-3′; reverse (1480–1499), 5′-CAGGA GCTAT GCTGC TCTTG-3′. The PCR products were cloned in the pGEM-T easy vector (Promega Corp., Madison, WI). The sense (SP6 RNA polymerase) and antisense (T7 RNA polymerase) riboprobes for *in situ* hybridization were synthesized in the presence of ^{35}S-uridine triphosphate (UTP) (NEN Life Science Products) or digoxigenin-UTP (Roche Molecular Biochemicals, Mannheim, Germany) by *in vitro* transcription.

In addition to the above probe, two 50-oligomer oligonucleotides, 1) 5′-GGAGC TAAAA CACTG GGGAC TGGGG GAGTA ATGTG TGGAA GGCCA CAAGAG-3′; and 2) 5′-CCTGC CACGC CTGTC TTTCT TTCCT AAGCC AGAGA AGTGG GGCAG CTGGA-3′, from the p29 sequence were used as probes in *in situ* hybridization experiments. The oligonucleotides were labeled with ^{35}S-α-deoxy-ATP (Dupont, Wilmington, DE) and terminal transferase (Roche Molecular Biochemicals).

A specific D2 antisense riboprobe was synthesized with SP6 RNA polymerase in the presence of ^{35}S-UTP (Dupont) using a 366-bp DNA template spanning nucleotides 535–901 (32) from the rat D2 cDNA sequence (5).

Northern blot analysis

The specificity of the probes was tested by Northern blot analysis with total RNA from cerebellum and cerebral cortex from P16 rats isolated as above. Northern blots were prepared using nylon membranes (Nytran, Schleicher & Schuell, Inc., Keene, NH). Ten micrograms of total RNA were fractionated on formaldehyde-agarose gels and transferred to the filters using standard techniques (36). The cDNA radioactive probes were labeled with the kit rediprime II (Amersham Pharmacia Biotech) using ^{32}P-deoxy-CTP. The filter was hybridized with the same probe used in the *in situ* hybridization analysis (327-bp probe spanning nucleotides 1172–1499 from the rat p29 cDNA). As control for the amount and integrity of the RNA present on the filters, blots were stained in 0.02% methylene blue solution in 0.3 M sodium acetate and then hybridized with a probe specific for the housekeeping gene glyceraldehyde-3-phosphate dehydrogenase.

In situ hybridization with radioactive probes

The detection of p29 and D2 mRNAs with ^{35}S-labeled riboprobes was performed on free-floating sections according to protocols previously described in detail (37, 38). Briefly, the sections were pretreated in different solutions for 10 min at room temperature each: permeabilized with 0.1% Triton X-100 in PBS, deproteinized with 0.2 N HCl, acetylated with 0.25% acetic anhydride in 0.1 M triethanolamine buffer (pH 8.0), postfixed in fixative, and washed in PBS. Prehybridization was performed at 55 C for 3–5 h, in a solution containing 50% formamide, 10% dextran sulfate, 5× Denhardt's solution, 0.62 M NaCl, 50 mM DTT, 0.01 M EDTA, 0.02 M 1,4-piperazinediethanesulfonic acid (pH 6.8), 0.2% sodium dodecyl sulfate, 250 μg/ml salmon sperm DNA, and 250 μg/ml yeast tRNA. Hybridization was performed in this solution at 55 C for 16 h, with the ^{35}S-labeled riboprobe at 1.6×10^7 cpm/ml. Excess probe was removed with 2× saline sodium citrate (SSC; 1× SSC is 0.015 M NaCl, 0.0015 M Na citrate) containing 10 mM β-mercaptoethanol at room temperature for 30 min, followed by incubation with 4 μg/ml ribonuclease A in 0.5 M NaCl, 0.05 M EDTA, 0.05 M Tris-HCl (pH 7.5) at 37 C for 1 h. Stringency washes were carried out in 0.5× SSC, 50% formamide, 10 mM β-mercaptoethanol at 55 C for 2 h, and then in 0.1× SSC, 10 mM β-mercaptoethanol at 68 C for 1 h.

To detect p29 mRNA with oligonucleotide probes, the free-floating sections were only acetylated, postfixed, and hybridized for 20 h at 42 C with ^{35}S-labeled oligonucleotides at 2×10^6 cpm/ml. Excess probe was removed with 1× SSC. Stringency washes were carried out in 1× SSC at 42 C and 0.1× SSC at room temperature.

In situ hybridization histochemistry and immunohistochemistry

To analyze the cell types that express p29 mRNA, a combination of *in situ* hybridization histochemistry and immunohistochemistry was performed in the same tissue section, using a double-labeling technique previously described (39). Briefly, after hybridization and washes, the free-floating sections were incubated sequentially with the primary antibody overnight at 4 C, then with a biotinylated secondary antibody (1:200, Vector Laboratories, Burlingame, CA) for 1 h at 4 C and finally processed by the avidin-biotin-peroxidase method using the Vectastain Elite ABC Kit (Vector Laboratories, PK-6100) with 0.05% 3,3′-diaminobenzidine tetrahydrochloride (Sigma, D-5905) and H_2O_2 as peroxidase substrates. Omitting the primary antibody resulted in negligible color development. The antibodies used were a polyclonal antibody against glial fibrillary acidic protein (1/2000; Dakopatts, M-0725) to detect astrocytes; a mouse monoclonal antibody antiparvalbumin (1/1000; Sigma, C-8666) and a mouse monoclonal antibody anticalbindin (1/4000; Sigma, C-9848) to localize subsets of interneurons.

Double in situ hybridization with riboprobes

For cellular colocalization studies, the free-floating sections were processed as described above but hybridized with both the p29-specific digoxigenin-labeled riboprobe at 200 ng/ml and the D2-specific ^{35}S-

labeled riboprobe at 1.6×10^7 cpm/ml. After several washes with PBS, the sections hybridized with digoxigenin-labeled riboprobe were preincubated with blocking solution, incubated with antidigoxigenin alkaline phosphatase conjugated antibody (1:5000, Roche) for 2 h and developed with 4-nitroblue tetrazolium–5-bromo-4-chloro-3-indolyl-phosphate (Roche) following the manufacturer's instructions.

Final processing

In all cases, the sections were mounted on coated slides, dehydrated, air-dried, and exposed to Kodak Biomax MR film (Eastman Kodak, Rochester, NY) for 6–12 d for p29 expression analysis and for 3 wk for colocalization studies. For cellular resolution, the sections were dipped in Hypercoat LM-1 photographic emulsion (Amersham Pharmacia Biotech), exposed for 20–30 d in the cold, developed with D19, fixed, dehydrated, and coverslipped. When only *in situ* hybridization was performed, the sections were counterstained with Richardson's blue.

Cytoarchitectonic analysis

The autoradiographic films were scanned in a Nikon Coolscan II slide scanner (Nikon Corp., Tokyo, Japan), at a resolution of 400 pixels/inch and printed. Optical observations and photographs were made in a Zeiss Axiophot microscope (Carl Zeiss, Oberkochen, Germany) and a Nikon digital camera Dn100. For the identification of brain structures, the atlas of Paxinos and Watson was followed (40).

Results

Regional distribution of p29 mRNA

Expression of p29 in rat brain was analyzed by *in situ* hybridization using a 327-nucleotide riboprobe synthesized from a DNA template encompassing nucleotides 1172–1499 from the published cDNA sequence. The probe hybridized to a 3.5-kb mRNA in Northern blots of cerebral cortex and cerebellum (Fig. 1A). Leonard *et al.* (22) reported a similar size mRNA in astrocytes. The distribution of p29 mRNA in brain slices obtained with this probe was identical to that using the oligonucleotide probes from other regions of the cDNA as described in the previous section (not shown). The data reported below were obtained using the 327-nucleotide riboprobe. A sense probe gave no signal (Fig. 1B).

p29 expression was analyzed in brains of euthyroid (Fig. 1, C1–C6) and hypothyroid (Fig. 1, D1–D6) rats on P16, an age when D2 expression and activity are highest in the brain (41). Further analysis using P60 euthyroid rats showed essentially the same pattern as on P16 (not shown). Briefly, highest p29 expression was found in the hippocampus, the neocortex, and the epithelial lining of the ventricles. p29 mRNA was also abundant in the choroid plexuses and the leptomeninges. Lower levels were found in the cerebellum and in several thalamic nuclei related to the reticular formation. White matter areas, such as the corpus callosum, were not labeled. The caudate and the olfactory bulb were almost devoid of p29 mRNA.

Looking at p29 expression in more detail, we found that in the cerebral cortex, p29 was mainly expressed in archicortex (hippocampus) and neocortex but hardly in paleocortex (olfactory cortex). In the hippocampus, there was an extremely high signal in the CA3 and CA4 regions of Ammon's horn, whereas CA1 and dentate gyrus were moderately labeled (Fig. 1, C4). Expression in the neocortex took place in all layers, except in layer I. There was a strong hybridization signal in layer IV and deep layer VI in frontal, agranular and parietal cortices (Fig. 1, C1–C4). However, in cingulate and retrosplenial cortices highest expression was localized in layer II. The piriform cortex showed little hybridization despite its high cellular density (Fig. 1, C2–C4).

It was noteworthy that a considerable hybridization signal was present in the lining of the ventricles, with the strongest signal in the third ventricle (Fig. 1, C4–C5). There was also significant hybridization signal in the other areas of the blood-CSF barrier: the choroid plexuses and the leptomeninges. Due to the floating hybridization technique, the leptomeninges were not well preserved in all the sections, but they appeared clearly labeled as shown in Fig. 1 (*arrows*). Other sites of p29 expression were the basolateral amygdaloid nucleus (Fig. 1, C4) and some nuclei related to the reticular formation (paraventricular, laterodorsal, reticular, and parafascicular thalamic nuclei; some of them are shown in Fig. 1, C4–C5). p29 was also expressed in the dorsal lateral geniculate nucleus and in the zona incerta (Fig. 1, C5). In the cerebellum, there was a higher signal in the internal granular layer and in the lining of the fourth ventricle. There was also an appreciable signal in the facial nuclei (Fig. 1, C6).

In previous studies, we found that D2 mRNA was increased in specific brain regions in response to hypothyroidism (31). Regarding p29, there was no difference in p29 expression in most regions (Fig. 1, D1–D6), except for a slightly increased signal in the choroid plexuses (Fig. 1, D3–D5).

To obtain microscopic resolution, we performed emulsion autoradiography and counterstained the sections. Figure 2 shows bright and dark field images (A–E and A′–E′, respectively) of relevant sites of p29 expression. In the somatosensory cortex (Fig. 2, A and A′), there was no signal in layer I and few silver grains in layers II–III, whereas layer V shows a medium label. The strongest radioactive signal was seen over layer IV and deep layer VI. In the hippocampus (Fig. 2, B, B′, C, and C′), there was a high density of silver grains in the pyramidal layers of the CA3 and CA4 regions, with much less hybridization signal in the granular layer of the dentate gyrus. There were also groups of silver grains that formed the shape of individual cellular somas in the polymorphic layer of the dentate gyrus; these cells were characterized as neurons (see next section).

There was a discrete signal over the lining of the third ventricle (Fig. 2, D and D′); the silver grains were located in the soma of ependymocytes and tanycytes and in their processes to the ventricle as shown at higher magnification in Fig. 2, E and E′. The autoradiographic analysis in hypothyroid rat brain showed an almost identical p29 expression to that found in normal brain (data not shown).

Cellular characterization of p29 expressing cells

The cells expressing p29 mRNA were characterized by analyzing their morphology and the expression of specific protein markers. To achieve this, we performed *in situ* hybridization combined with Nissl staining or with immunohistochemistry in the same tissue slice. We used antibodies against glial fibrillary acidic protein expressed mainly by astroglial cells, and against calbindin and parvalbumin expressed by subpopulations of interneurons.

Besides expression in ependymocytes and tanycytes, as

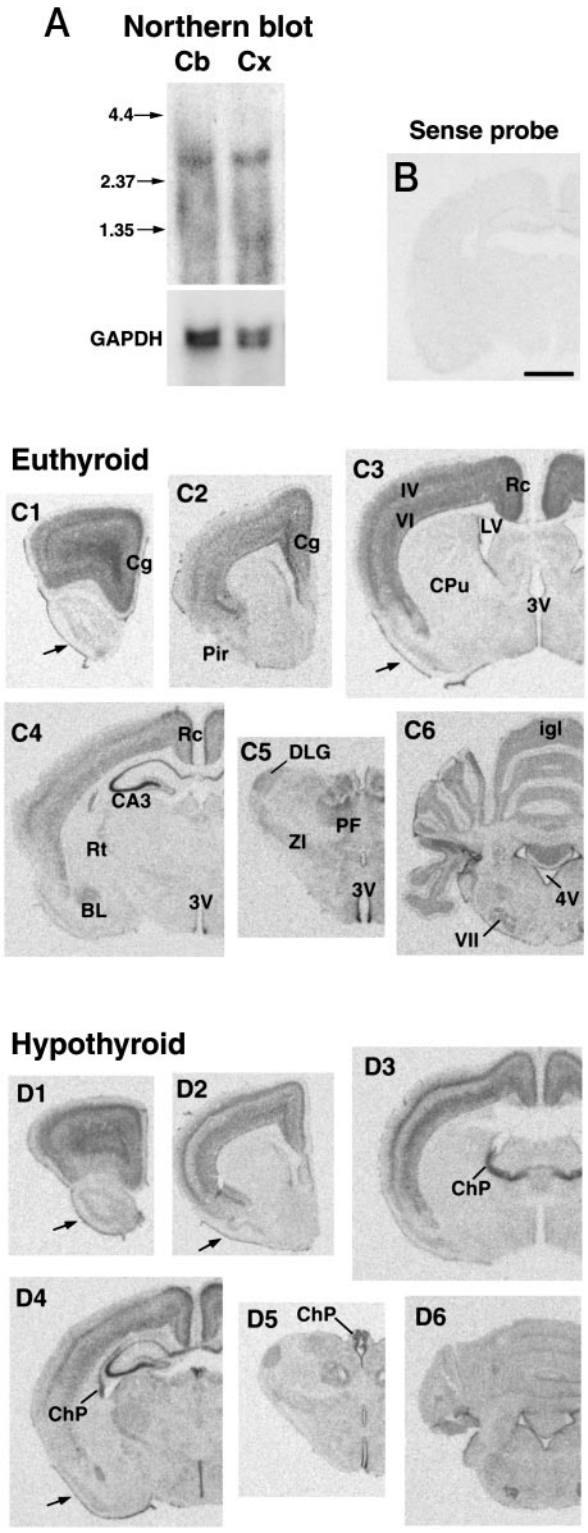

FIG. 1. Regional expression of p29 in brain of normal and hypothyroid rats. A, Northern blot of p29 in the cerebellum (Cb) and cerebral cortex (Cx); the *arrows* show the size of RNA standards. The size of the p29 band was read from the regression line obtained in a semilog plot of standard mRNA sizes *vs.* distance migrated in the electrophoresis gel. A glyceraldehyde-3-phosphate dehydrogenase probe was used for control of RNA loading. B, Brain slice hybridized with a sense riboprobe. In panels C and D, the sections are organized from anterior to posterior levels. C1–C6, Expression of p29 in slices from an euthyroid rat. D1–D6, Expression in a hypothyroid rat. Cg, Cingulated cortex; Pir, piriform cortex; IV and VI, layers of the neocortex; Rc, retrosplenial cortex; LV lateral ventricle; CPu, caudate-putamen; CA3, field 3 of Ammon's horn; Rt, reticular thalamic nucleus; BL, basolateral amygdaloid nucleus; 3V and 4V, third and fourth ventricles; PF, parafascicular nucleus; DLG, dorsolateral geniculate nucleus; ZI, zona incerta; igl, internal granular layer; VII, facial nucleus; ChP, choroid plexuses. *Arrows* in C1, C3, D1, D2, and D4 point to the meninges. *Scale bar*, 0.2 cm.

mentioned above, the data indicate that p29 is expressed in neurons, mainly pyramidal neurons. As shown above, p29 expression in the hippocampus took place mainly in pyramidal layers. This was confirmed by emulsion photography that showed the hybridization grains over pyramidal cells (Fig. 3A). Also in the neocortex, the silver grains were associated to neurons. p29 expression was strong in layer IV and deep layer VI. In layer IV and VI, the grains were aggregated resembling round shapes of large and medium sizes (Fig. 3B). Many calbindin positive interneurons express p29 in layer IV and some of them in layer VI (Fig. 3E) and in the polymorphic layer of the dentate gyrus. However, the parvalbumin immunopositive cells in the neocortex did not contain silver grains (Fig. 3F). Neuronal expression of p29 was also strongly supported by the finding of silver grains over large neurons of the reticular formation giganto cellularis in the medulla (Fig. 3C). The white matter was devoid of p29 mRNA, and there was no signal over oligodendrocytes recognized by their morphology and disposition in linear arrays (Fig. 3B). Figure 3D shows p29 expression in ependymocytes and the choroid plexus.

Lack of colocalization of p29 and D2 mRNAs

To assess a possible functional relationship between p29 and D2, we examined whether or not both molecules were simultaneously present in some subsets of cells. To this end, we used a D2 radioactive probe together with a p29 probe labeled with digoxigenin. The mixed probes were used for *in situ* hybridization on P16 brain slices. Regional expression of D2 was identical to that previously reported (31). As was expected from the results described above regarding p29 expression, both mRNAs were located in different cellular groups throughout the brain. At the regional level, D2 was expressed in some regions which lack p29, such as the caudate, whereas others, such as the amygdala expressed p29 but not D2 (not shown). D2 was not expressed in the ependymocytes lining the ventricles, the leptomeninges, and the choroid plexuses, places with prominent p29 expression (Fig. 1).

In other regions, such as the neocortex and the hippocampus both mRNAs were expressed, but in different layers or cell types. Figure 4, A and A′, shows that layer I of the neocortex expressed D2 but not p29, which was present in neurons at the upper border of layer II. These neurons did not express D2. In the hippocampus, D2 was clearly present in the molecular layer of the dentate gyrus, where it was expressed in astrocytes, whereas p29 was expressed in the granular and pyramidal layers (Fig. 4, B and B′).

The only cells that appeared to express both mRNAs were the tanycytes, a specialized type of glial cells, which replace the ependymocytes in the bottom of the third ventricle (Fig.

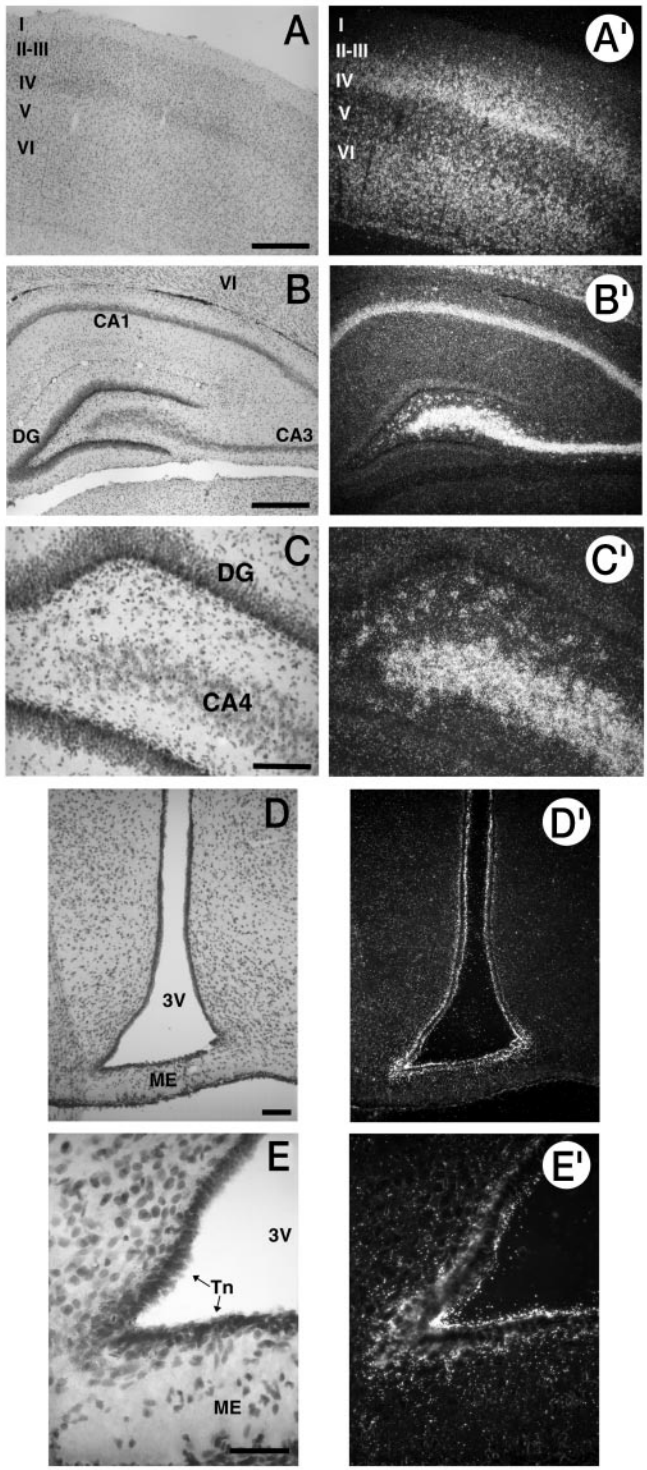

FIG. 2. Bright field (*left panels*) and dark field (*right panels*) microphotographs of p29 expression. *In situ* hybridization was performed using a p29 radioactively labeled riboprobe. After hybridization, the sections were covered with photographic emulsion, exposed, and developed to reveal the silver grains (*white signal in right panels*). The sections were then counterstained to reveal the cellular distribution (*left panels*). Layers of cerebral neocortex are labeled I to VI. DG, Dentate gyrus; CA1–4, fields of Ammon's horn; Po, polymorphic layer of the dentate gyrus; 3V, third ventricle; ME, median eminence; Tn, tanycytes. *Scale bars* in A and B, 500 μm; in C and D, 100 μm; and in E, 50 μm.

4, C and C′). The tanycytes are the cells with the highest D2 expression in brain (32, 33). However, whereas p29 mRNA was present mainly in the tanycyte bodies, D2 was present in the tanycyte processes, and their feet near the median eminence. In the median eminence, p29 expression was high in the leptomeninges (Fig. 4, C and C′).

Discussion

The goal of this work was to explore a possible functional relationship between D2 and the putative T_4-binding protein p29 *in vivo*. Studies *in vitro* indicate that p29 overexpression increases D2 activity 100 times, and the use of specific antibodies against p29 led to inmunoprecipitation of 5′-deiodinase activity both in astrocyte cultures and in microsomal fractions isolated from hypothyroid BAT and cerebral neocortex. In addition, direct injection of recombinant Ad5-p29 virus particles in the neocortex slightly increased (2×) 5′-deiodinase activity (22).

As an initial approach, we performed *in situ* hybridization studies to determine whether the two genes were expressed in the same groups of cells in the brain. Studying mRNA distribution has obvious limitations. However, the study of D2 protein distribution is hampered by lack of antibodies suitable for immunohistochemistry and probably extremely low cellular concentrations of the protein. Nevertheless, the regional heterogeneity of the central nervous system allows inferring the existence of functional relationships among different molecules from expression correlates. As described previously, D2 was mainly expressed in the tanycytes lining the inferior walls of the third ventricle, and also in brain structures such as the cerebral neocortex, hippocampus, caudate, midbrain, brain stem, and cerebellum (32, 33). p29 was expressed in the neocortex, hippocampus, cerebellum, amygdala, and some thalamic nuclei related to the reticular formation. It was absent from the caudate, one of the regions were D2 is expressed. Other sites of prominent p29 expression include the leptomeninges, the epithelial cells of the choroid plexuses, the ependimocytes, and the tanycytes. In regions where both D2 and p29 were expressed, they were present in different layers or in different groups of cells. D2 is expressed in astrocytes (32), whereas p29 is localized in neurons. The only cells that appeared to coexpress both mRNAs were the tanycytes, but given the lack of coexpression elsewhere, it is doubtful that the eventual presence of both proteins in the tanycytes reflects any functional relation between them.

D2 expression in rat brain is influenced by developmental and physiological factors. Enzyme activity and mRNA abundance are highest during the postnatal period than in fetal life and are also regulated by the thyroidal status. Hypothyroidism induced an increase in D2 activity in total brain and cerebral cortex (27, 28, 30). Iodine deficiency also increased D2 mRNA and activity in brain (29, 42). As we have shown previously, profound hypothyroidism induced an increased D2 mRNA in the relay nuclei of somatosensory and auditory pathways, which could be thought as being especially protected from low T_3 by an increased D2 activity (31). D2 mRNA expression also increases severalfold in the tanycytes after hypothyroidism (33). In contrast, except for a slightly

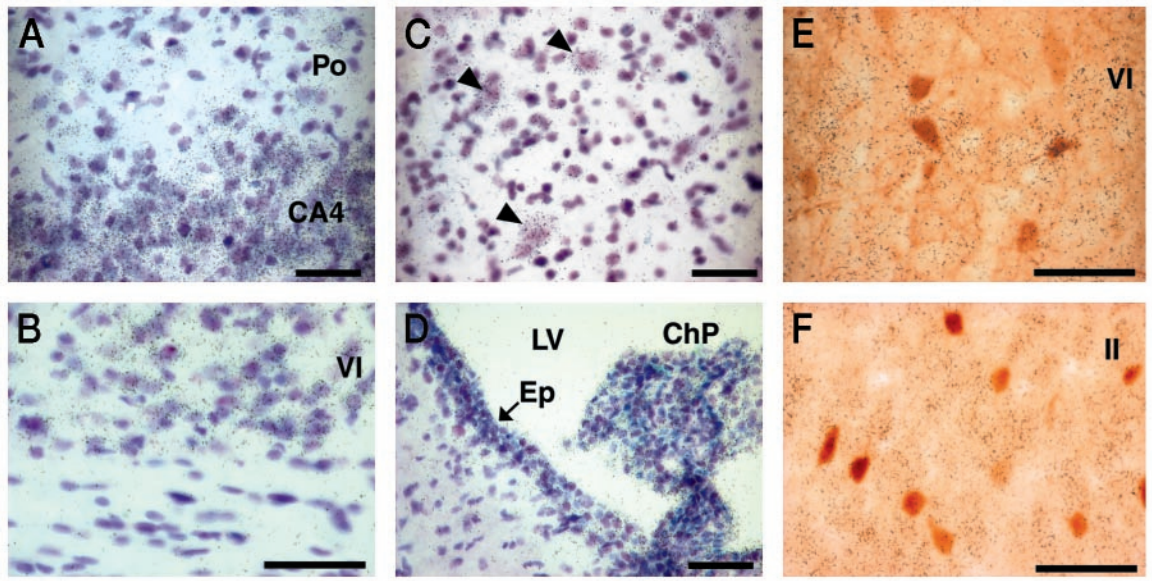

FIG. 3. Expression of p29 at the cellular level. *In situ* hybridization using emulsion microphotograpy was combined with Nissl staining (A–D) or with immunohistochemistry with specific antibodies for calbindin (E) or parvalbumin (F). Po, Polymorphic layer of the dentate gyrus; CA4, field of the Ammon's horn; II and VI, layers of the cerebral neocortex; LV, lateral ventricle; ChP, choroid plexus; Ep, ependymocytes. *Arrowheads* point to giant neurons in the reticular formation giganto cellularis. *Scale bars*, 100 μm.

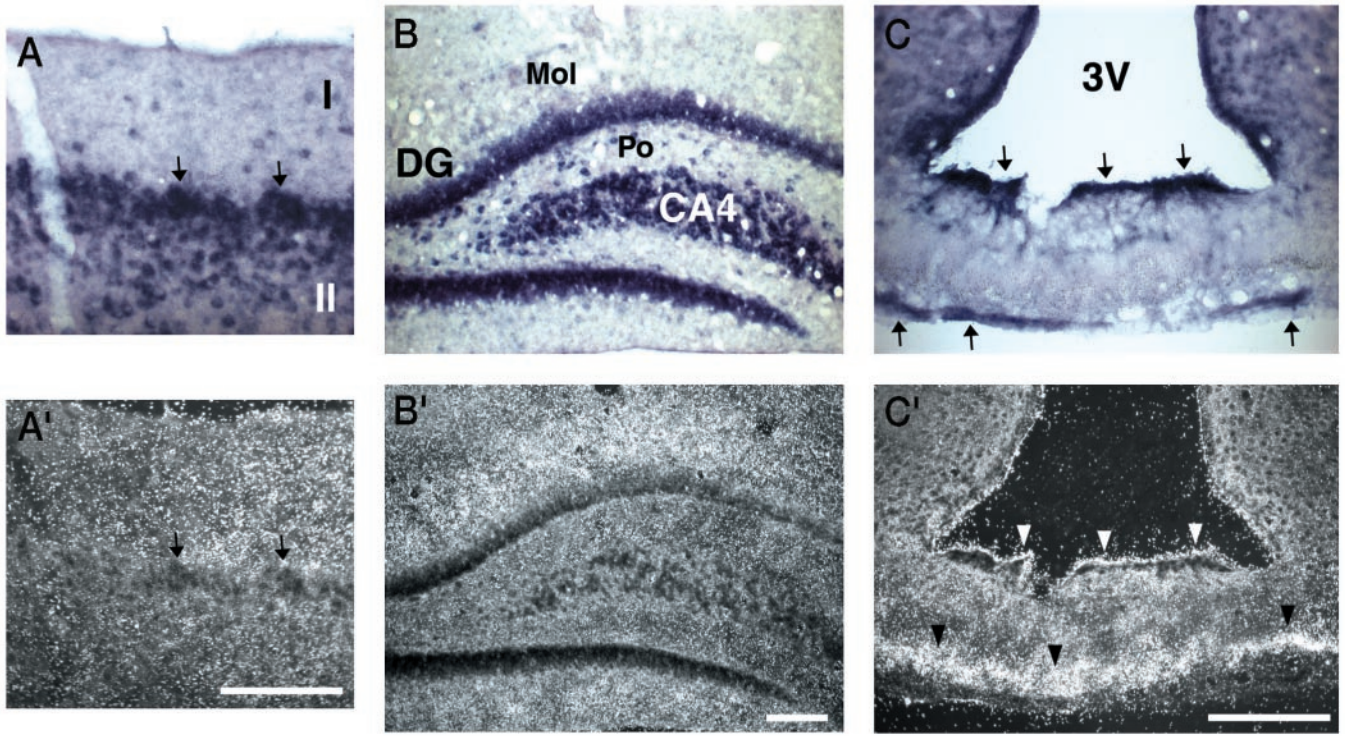

FIG. 4. Simultaneous detection of p29 and D2 mRNAs. Double *in situ* hybridization with a p29 digoxigenin-labeled riboprobe (*blue staining*) and a D2 radioactively labeled riboprobe (hybridization grains). The *upper panels* show bright-field, and the *lower panels*, dark-field images. I–II, Layers of retrosplenial cortex; DG, dentate gyrus; CA4, field of Ammon's horn; Po, polymorphic layer of the dentate gyrus; Mol, molecular layer of the dentate gyrus. *Arrows* point to p29 mRNA signal in layer II of the retrosplenial cortex and in tanycytes somas and in meninges. *Arrowheads* point to D2 mRNA signal in tanycytes somas (*white*) and tanycytes feet (*black*) at the median eminence. *Scale bars*, 150 μm.

increased expression of p29 in the choroid plexuses, expression of p29 was not altered by hypothyroidism in most regions.

It is intriguing that p29 was expressed all along the whole cell layer covering the ventricles, as ependimocytes and tanycytes, and also forming the epithelial layer of the choroid plexuses and the arachnoid membrane. The mechanisms of T_4 transport in the brain are at present not well understood.

Both T_4 and T_3 can enter the brain through the blood-brain and the cerebrospinal fluid-brain barriers (43). The passage through the blood-CSF barrier, *i.e.* through the epithelial cells lining the ventricular side of the choroid plexus, was thought to be facilitated by locally synthesized transthyretin. However, results from transthyretin knockout animals do not support this hypothesis (44, 45). p29 was originally identified as a putative T_4-binding protein (15). If indeed p29 binds T_4 *in vivo*, then its expression in cells lining the brain-CSF interface may suggest a function of p29 in T_4 transport to and from the CSF. More studies are clearly needed to explore this possibility.

Rat p29 shows very high sequence similarity with mouse Dkk-3, a member of the Dikkopf protein family, which have a role during *Xenopus* development (23). Given their high sequence similarity, p29 might be considered as the rat homolog of Dkk-3. In fact, the p29 sequence appears in the GenBank database defined as the rat Dkk-3 homolog with accession no. NM_138519. On the other hand, the derived protein sequence lacks the signal peptide that makes all Dickkopf family members secreted glycoproteins. Close comparison of the reported p29 sequence with that of mouse Dkk-3, however, reveals a high sequence similarity, with conserved nucleotide substitutions also in the region encoding the Dkk-3 signal peptide. Dkk-3 is expressed in the ventricular zones of developing brain and spinal chord (24), resembling the ventricular localization of p29 found in the postnatal rat brain. Although expression of mouse Dkk-3 has not been studied in detail, in the adult it is expressed in the hippocampus and cerebral neocortex in a pattern very similar to that described for p29 in our work (23).

In summary, we found that in most regions of the brain p29 and D2 show dissimilar distributions. This argues against the hypothesis that p29 is part of a D2 multienzyme complex. Related functions for p29, such as a role in T_4 transport, cannot be discarded. Such a role would be compatible with its prominent expression in cells lining the choroid plexuses and the walls of the ventricles.

Acknowledgments

We acknowledge Drs. Javier DeFelipe and Estrella Rausell for helpful discussion and interpretation of results; Fernando Núñez, Pablo Señor, and Miguel Marsa for the care of animals; and Luis Almonacid for technical help.

Received August 7, 2002. Accepted November 7, 2002.

Address all correspondence and requests for reprints to: Dr. Juan Bernal, Instituto de Investigaciones Biomédicas, Arturo Duperier 4, 28029 Madrid, Spain. E-mail: jbernal@iib.uam.es.

This work was supported by Grants PM980118 and BFI2001-2412 from Ministerio de Ciencia y Tecnología, and QLG3-2000-00930 from the European Union. A.M.-P. is recipient of a fellowship from the Ministry of Science and Technology, Spain. A.G.-F. is recipient of a contract from the Ramón y Cajal Program of the Ministry of Science and Technology, Spain.

References

1. **Bianco AC, Salvatore D, Gereben B, Berry MJ, Larsen PR** 2002 Biochemistry, cellular and molecular biology, and physiological roles of the iodothyronine selenodeiodinases. Endocr Rev 23:38–89
2. **Leonard JL, Köhrle J** 2000 Intracellular pathways of iodothyronine metabolism. In: Braverman LE, Utiger RD, eds. Werner and Ingbar's the thyroid: a fundamental and clinical text. 8th ed. Philadelphia: Lippincott Williams and Wilkins; 136–173
3. **Köhrle J** 1999 Local activation and inactivation of thyroid hormones: the deiodinase family. Mol Cell Endocrinol 151:103–119
4. **Leonard JL, Visser TJ** 1986 Biochemistry and deiodination. In: Hennemann G, ed. Thyroid hormone metabolism. New York: Marcel Dekker Inc.; 189–229
5. **Croteau W, Davey JC, Galton VA, St. Germain DL** 1996 Cloning of the mammalian type II iodothyronine deiodinase: a selenoprotein differentially expressed and regulated in the human brain and other tissues. J Clin Invest 98:405–417
6. **Berry MJ, Larsen PR** 1993 Molecular cloning of the selenocysteine-containing enzyme type I iodothyronine deiodinase. Am J Clin Nutr 57(Suppl 2):249–255
7. **Croteau W, Whittemore SL, Schneider MJ, St. Germain DL** 1995 Cloning and expression of a cDNA for a mammalian type III iodothyronine deiodinase. J Biol Chem 270:16569–16575
8. **Salvatore D, Bartha T, Harney JW, Larsen PR** 1996 Molecular biological and biochemical characterization of the human type 2 selenodeiodinase. Endocrinology 137:3308–3315
9. **St Germain DL, Galton VA** 1997 The deiodinase family of selenoproteins. Thyroid 7:655–668
10. **Berry MJ, Banu L, Chen YY, Mandel SJ, Kieffer JD, Harney JW, Larsen PR** 1991 Recognition of UGA as a selenocysteine codon in type I deiodinase requires sequences in the 3′ untranslated region. Nature 353:273–276
11. **Mandel SJ, Berry MJ, Kieffer JD, Harney JW, Warne RL, Larsen PR** 1992 Cloning and *in vitro* expression of the human selenoprotein, type I iodothyronine deiodinase. J Clin Endocrinol Metab 75:1133–1139
12. **Buettner C, Harney JW, Larsen PR** 1998 The 3′-untranslated region of human type 2 iodothyronine deiodinase mRNA contains a functional selenocysteine insertion sequence element. J Biol Chem 273:33374–33378
13. **Curcio C, Baqui MM, Salvatore D, Rihn BH, Mohr S, Harney JW, Larsen PR, Bianco AC** 2001 The human type 2 iodothyronine deiodinase is a selenoprotein highly expressed in a mesothelioma cell line. J Biol Chem 276:30183–30187
14. **Schneider MJ, Fiering SN, Pallud SE, Parlow AF, St. Germain DL, Galton VA** 2001 Targeted disruption of the type 2 selenodeiodinase gene (DIO2) results in a phenotype of pituitary resistance to T_4. Mol Endocrinol 15:2137–2148
15. **Farwell AP, Leonard JL** 1989 Identification of a 27-kDa protein with the properties of type II iodothyronine 5′-deiodinase in dibutyryl cyclic AMP-stimulated glial cells. J Biol Chem 264:20561–20567
16. **Safran M, Farwell AP, Leonard JL** 1996 Catalytic activity of type II iodothyronine 5′-deiodinase polypeptide is dependent upon a cyclic AMP activation factor. J Biol Chem 271:16363–16368
17. **Safran M, Farwell AP, Leonard JL** 1991 Evidence that type II 5′-deiodinase is not a selenoprotein. J Biol Chem 266:13477–13480
18. **Chanoine JP, Safran M, Farwell AP, Tranter P, Ekenbarger DM, Dubord S, Alex S, Arthur JR, Beckett GJ, Braverman LE, Leonard JL** 1992 Selenium deficiency and type II 5′-deiodinase regulation in the euthyroid and hypothyroid rat: evidence of a direct effect of thyroxine. Endocrinology 131:479–484
19. **Salvatore D, Harney JW, Larsen PR** 1999 Mutation of the Secys residue 266 in human type 2 selenodeiodinase alters 75Se incorporation without affecting its biochemical properties. Biochimie (Paris) 81:535–538
20. **Berry MJ, Kieffer JD, Larsen PR** 1991 Evidence that cysteine, not selenocysteine, is in the catalytic site of type II iodothyronine deiodinase. Endocrinology 129:550–552
21. **Leonard JL, Leonard DM, Safran M, Wu R, Zapp ML, Farwell AP** 1999 The mammalian homolog of the frog type II selenodeiodinase does not encode a functional enzyme in the rat. Endocrinology 140:2206–2215
22. **Leonard DM, Stachelek SJ, Safran M, Farwell AP, Kowalik TF, Leonard JL** 2000 Cloning, expression, and functional characterization of the substrate binding subunit of rat type II iodothyronine 5′-deiodinase. J Biol Chem 275: 25194–25201
23. **Krupnik VE, Sharp JD, Jiang C, Robison K, Chickering TW, Amaravadi L, Brown DE, Guyot D, Mays G, Leiby K, Chang B, Duong T, Goodearl AD, Gearing DP, Sokol SY, McCarthy SA** 1999 Functional and structural diversity of the human Dickkopf gene family. Gene 238:301–313
24. **Monaghan AP, Kioschis P, Wu W, Zuniga A, Bock D, Poustka A, Delius H, Niehrs C** 1999 Dickkopf genes are co-ordinately expressed in mesodermal lineages. Mech Dev 87:45–56
25. **Tsuji T, Miyazaki M, Sakaguchi M, Inoue Y, Namba M** 2000 A REIC gene shows down-regulation in human immortalized cells and human tumor-derived cell lines. Biochem Biophys Res Commun 268:20–24
26. **Bernal J** 2002 Action of thyroid hormone in brain. J Endocrinol Invest 25: 268–288
27. **Leonard JL, Kaplan MM, Visser TJ, Silva JE, Larsen PR** 1981 Cerebral cortex responds rapidly to thyroid hormones. Science 214:571–573
28. **Silva JE, Gordon MB, Crantz FR, Leonard JL, Larsen PR** 1984 Qualitative and quantitative differences in the pathways of extrathyroidal triiodothyronine generation between euthyroid and hypothyroid rats. J Clin Invest 73:898–907
29. **Obregón MJ, Ruiz de Oña C, Calvo R, Escobar del Rey F, Morreale de Escobar G** 1991 Outer ring iodothyronine deiodinases and thyroid hormone economy: responses to iodine deficiency in the rat fetus and neonate. Endocrinology 129:2663–2673

30. **Escobar-Morreale HF, Obregon MJ, Hernandez A, Escobar del Rey F, Morreale de Escobar G** 1997 Regulation of iodothyronine deiodinase activity as studied in thyroidectomized rats infused with thyroxine or triiodothyronine. Endocrinology 138:2559–2568
31. **Guadaño-Ferraz A, Escámez MJ, Rausell E, Bernal J** 1999 Expression of type 2 iodothyronine deiodinase in hypothyroid rat brain indicates an important role of thyroid hormone in the development of specific primary sensory systems. J Neurosci 19:3430–3439
32. **Guadaño-Ferraz A, Obregón MJ, St-Germain D, Bernal J** 1997b The type 2 iodothyronine deiodinase is expressed primarily in glial cells in the neonatal rat brain. Proc Natl Acad Sci USA 94:10391–10396
33. **Tu HM, Kim SW, Salvatore D, Bartha T, Legradi G, Larsen PR, Lechan RM** 1997 Regional distribution of type 2 thyroxine deiodinase messenger ribonucleic acid in rat hypothalamus and pituitary and its regulation by thyroid hormone. Endocrinology 138:3359–3368
34. **Riskind PN, Kolodny JM, Larsen PR** 1987 The regional hypothalamic distribution of type II 5′-monodeiodinase in euthyroid and hypothyroid rats. Brain Res 420:194–198
35. **Morte B, Manzano J, Scanlan T, Vennström B, Bernal J** 2002 Deletion of the thyroid hormone receptor 1 prevents the structural alterations of the cerebellum induced by hypothyroidism. Proc Natl Acad Sci USA 99:3985–3989
36. **Sambrook J, Fritsch EF, Maniatis T** 1989 Molecular cloning: a laboratory manual. Plainview, NY: Cold Spring Harbor Laboratory Press
37. **Iñiguez MA, De Lecea L, Guadaño-Ferraz A, Morte B, Gerendasy D, Sutcliffe JG, Bernal J** 1996 Cell-specific effects of thyroid hormone on RC3/neurogranin expression in rat brain. Endocrinology 137:1032–1041
38. **Bernal J, Guadaño-Ferraz A** 2002 Analysis of thyroid hormone-dependent genes in the brain by in situ hybridization. Methods Mol Biol 202:71–90
39. **Guadaño-Ferraz A, Escámez MJ, Morte B, Vargiu P, Bernal J** 1997 Transcriptional induction of RC3/neurogranin by thyroid hormone: differential neuronal sensitivity is not correlated with thyroid hormone receptor distribution in the brain. Mol Brain Res 49:37–44
40. **Paxinos G, Watson C** 1986 The rat brain in stereotaxic coordinates. London: Academic Press, Inc.
41. **Kaplan MM, Yaskoski KA** 1981 Maturational patterns of iodothyronine phenolic and tyrosyl ring deiodinase activities in rat cerebrum, cerebellum, and hypothalamus. J Clin Invest 67:1208–1214
42. **Peeters R, Fekete C, Goncalves C, Legradi G, Tu HM, Harney JW, Bianco AC, Lechan RM, Larsen PR** 2001 Regional physiological adaptation of the central nervous system deiodinases to iodine deficiency. Am J Physiol Endocrinol Metab 281:E54–E61
43. **Dratman MB, Crutchfield FL, Schoenhoff MB** 1991 Transport of iodothyronines from bloodstream to brain: contributions by blood:brain and choroid plexus:cerebrospinal fluid barriers. Brain Res 554:229–236
44. **Palha JA, Fernandes R, de Escobar GM, Episkopou V, Gottesman M, Saraiva MJ** 2000 Transthyretin regulates thyroid hormone levels in the choroid plexus, but not in the brain parenchyma: study in a transthyretin-null mouse model. Endocrinology 141:3267–3272
45. **Palha JA, Hays MT, Morreale de Escobar G, Episkopou V, Gottesman ME, Saraiva MJ** 1997 Transthyretin is not essential for thyroxine to reach the brain and other tissues in transthyretin-null mice. Am J Physiol 272:E485–E493